JOURNAL OF MATERIALS SCIENCE 28 (1993) 6631–6638

High-temperature strength and fracture toughness in γ-phase titanium aluminides

R. GNANAMOORTHY, Y. MUTOH
Department of Mechanical Engineering, Nagaoka University of Technology, Nagaoka-shi 940-21, Japan
N. MASAHASHI
Nippon Steel Corporation, Nakahara-ku, Kawasaki 211, Japan
M. MATSUO
JATIS, Chiyoda-ku, Tokyo 100, Japan

High-temperature strengths and fracture toughnesses of γ-phase titanium aluminides were estimated at room and elevated temperatures. The effects of chromium on these mechanical properties were investigated. It was found that addition of chromium substantially improved the room- and high-temperature strength and toughness of the binary titanium aluminides. The transition temperature at which the strength drops was found to increase due to the addition of chromium. The fracture behaviour of binary and chromium-alloyed titanium aluminides were investigated. The fracture mechanism was affected by the addition of chromium. Ductile tearing was observed for the ternary material at 800 °C, and this was delayed for the binary material.

1. Introduction

The light weight and the excellent high-temperature properties of titanium-aluminide-based intermetallic compounds make them most suitable for elevated–temperature applications [1–3]. Among titanium aluminides, γ-phase materials are of special interest because they have higher oxidation resistance, higher elastic modulus and better creep properties than α_2-phase titanium aluminides. But, their low room-temperature ductility and poor formability restrict any industrial applications. Addition of ternary elements such as chromium [4], manganese [5] and vanadium [6] was found to have a considerable influence on the mechanical properties of titanium aluminides. Two-phase alloys have shown high ductility up to 2.2% in binary alloys (Ti–48Al) [7] and as high as 4% in ternary alloys (Ti–48Al–(1–2)Mn, Cr, V) [8]. Still, the maximum room-temperature ductility and toughness achieved are below the acceptable limits for practical applications. A better understanding of the fracture mechanism and the characteristic values of the fracture toughness are necessary for designing alloys with improved ductility and toughness. The fracture mechanism of binary titanium aluminides has been investigated in detail [9–12]. However, the fracture mechanism of ternary titanium aluminides with improved mechanical properties has not yet been studied in detail.

The fracture-mechanics approach has not been developed fully in the research field of intermetallic compounds. So, valid fracture-toughness values (estimated by the standard test procedures [13, 16]) are not available for these materials at elevated temperatures. A low yield strength, compared to the fracture toughness, makes fracture-toughness estimation more complicated at room and high temperatures. Thick specimens are needed to estimate the fracture-toughness values, K_{Ic}, in accordance with the ASTM standard [13]. Many investigators have shown that the ductility of titanium-based intermetallic compounds increases drastically with increasing temperature [7, 14, 15]. This will increase the fracture toughness at higher temperatures. So, it will be very difficult to obtain the K_{Ic} fracture-toughness values, since fracture will occur after a large amount of plastic deformation and stable crack growth at elevated temperatures. So, it is essential to estimate the fracture toughness using the elastic–plastic fracture parameter, the J-Integral [16]. The standard test procedure of estimating the elastic–plastic fracture toughness, J_{Ic}, requires too many specimens [16].

In the present study, a simple test procedure, using a single specimen with a side-groove, was followed to estimate the acceptable values of fracture toughness at room and elevated temperatures for the binary TiAl and chromium-alloyed TiAl. The fracture mechanisms at room and elevated temperatures were investigated. The effects of chromium addition on the strength, the fracture toughness and the fracture mechanism are discussed.

2. Materials and experimental procedure

2.1. Test materials

This investigation used γ-based Ti–50 at % Al and Ti–47 at % Al–3 at% Cr, which are referred to as TiAl and TiAlCr, respectively. High-purity ingots were prepared by plasma arc melting. The nominal compositions of the test materials are shown in Table I. The ingots were homogenized for 96 h at 1050 °C in vacuum. The cast and homogenized microstructures of the test materials are shown in Fig. 1. The homogenized TiAl was mostly γ-phase with very little α_2-phase. The mean grain size was about 200 μm. The homogenized TiAlCr contained mostly equiaxed grains. Some lamellar grains were also observed. X-ray diffraction (XRD) studies carried out on the heat-treated TiAlCr samples indicated the presence of the β-phase (body-centred cubic b.c.c.) in addition to the α_2-phase and γ-phase. Detailed transmission electron microscopy (TEM) investigations performed by Hanamura *et al.* [17] also confirmed the presence of the β-phase (b.c.c.) in heat-treated TiAlCr. The mean grain size of the TiAlCr was about 60 μm. Test specimens were made by multi-wire cutting followed by machining to the required dimensions and surface finish.

TABLE I Chemical compositions of the test materials

Alloy	Composition (at (%)			Composition (p.p.m)		
	Ti	Al	Cr	O	H	C
TiAl	49.1	50.9	–	170	5.0	70
TiAlCr	48.1	49.2	2.75	250	7.0	120

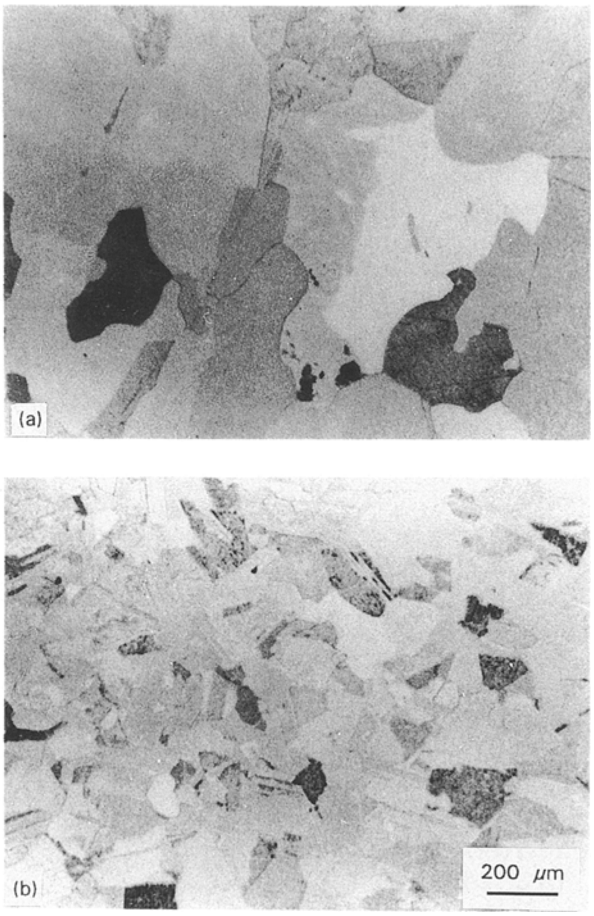

Figure 1 Optical micrographs of the test materials: (a) TiAl, and (b) TiAlCr.

2.2. Experimental procedure

2.2.1. Flexural-strength experiments

The flexural strengths of the test materials were estimated using three-point-bend specimens of dimensions $3 \times 4 \times 35\ mm^3$ (Fig. 2a) at room and elevated temperatures in a vacuum of better than 4×10^{-3} Pa. The span length of the three-point bending was 30 mm. Experiments were conducted with an Instron-type universal testing machine at a crosshead speed of $0.5\ mm\ min^{-1}$. The specimens were soaked at the test temperature for at least 15 min before testing. Fractographical investigations were carried out on the fractured surfaces by scanning electron microscopy (SEM).

2.2.2. Fracture-toughness experiments

Initially, fracture-toughness tests using specimens of dimensions $5 \times 10 \times 55\ mm^3$ were carried out to estimate the K_Q fracture-toughness value for the binary TiAl. From the estimated values, it was found that thicker specimens were needed to estimate the plane-strain-fracture-toughness values for these materials. So, a simple J_{Ic} test method using a side-grooved specimen was followed for the rest of the experiments to estimate the fracture toughness, J_{Ic}, at room and elevated temperatures. The maximum load in the load–displacement plot of the specimens with proper depths of the side-groove and precrack coincided with the crack-initiation point [18].

An electro-discharge-machine (EDM) notch was machined in three-point-bend specimens (Fig. 2b) as a starter for fatigue precracking. The fatigue precrack was introduced up to an a/W ratio of about 0.5 using a sinusoidal wave at 10 Hz and a stress ratio of 0.1. The final maximum stress-intensity factor for fatigue cracking, K_{fmax}, was controlled lower than $0.6K_{Ic}$. A side-groove was introduced in the precracked specimens using a fine diamond cutter of 0.3 mm thickness to a depth of about 25% of the specimen thickness. This precrack length and side-groove depth made the maximum-load point coincide with the crack-initiation point [19].

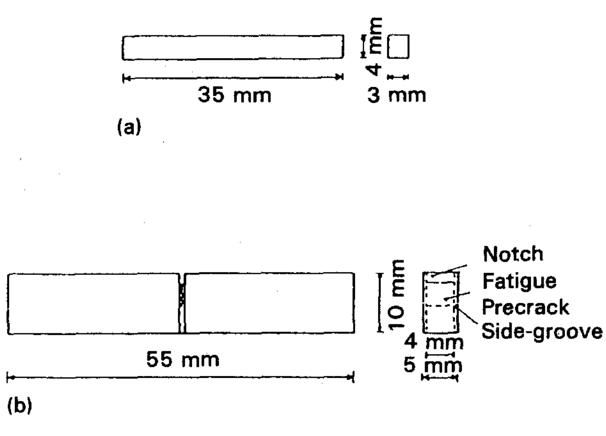

Figure 2 Geometry of the test specimens (all dimensions are in mm): (a) three-point-bend specimen, and (b) side-grooved toughness specimen.

Fracture-toughness experiments were carried out with an Instron-type universal testing machine at a crosshead speed of 0.5 mm min^{-1} in a vacuum of better than 4×10^{-3} Pa. The span length of the three-point bending was 40 mm. Specimens were soaked at the test temperature for 15 min before testing. After testing, the fracture surfaces were studied by SEM.

3. Results

3.1. Flexural strength

3.1.1. *TiAl*

Fig. 3 shows the relationship between flexural strength and temperature for the test materials. For the binary TiAl, the room temperature strength was low and increased with temperature up to 600 °C. Above 600 °C, the flexural strength decreased. At room temperature, the fracture surface exhibited a transgranular-cleavage mode of fracture with typical "river-patterns" as shown in Fig. 4a. Marks of twin and/or slip lines were observed on quasi-cleavage fracture surfaces of the specimens fractured at 600 °C (Fig. 4b). Specimens tested at 800 and 1000 °C were very ductile and did not fracture. The fracture surfaces of the specimens bent at 800 and 1000 °C and subsequently fractured at room temperature represented the room-temperature fracture modes.

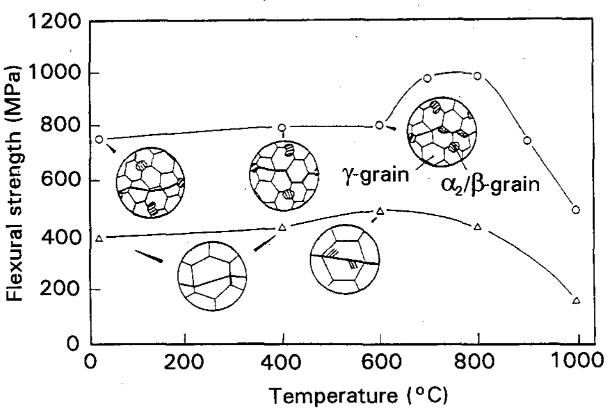

Figure 3 Flexural strength versus temperature for test materials with a schematic of the dominant fracture mode: (△) TiAl, and (○) TiAlCr.

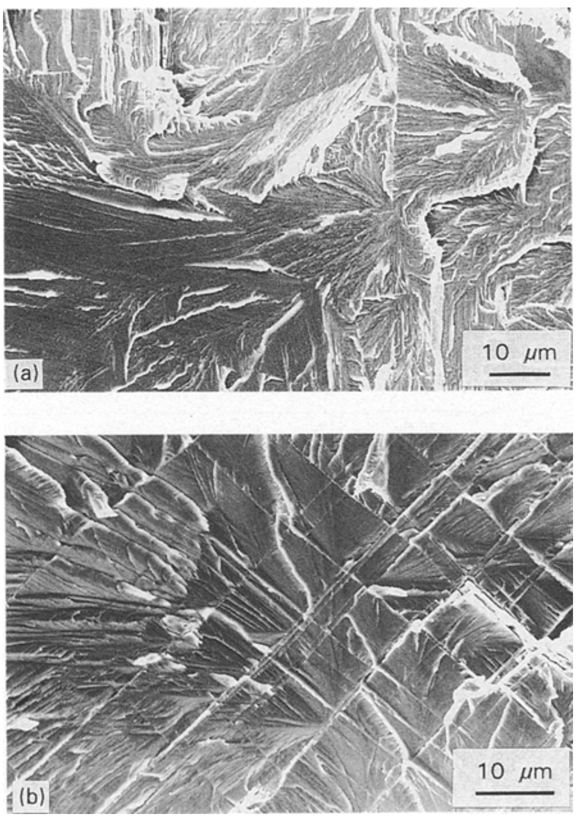

Figure 4 SEM fractographs of TiAl bend specimens: (a) 20 °C, and (b) 600 °C.

3.1.2. *TiAlCr*

The flexural strength of TiAlCr was very high at both room and elevated temperatures compared to binary TiAl. An inverse temperature dependency of strength, which was similar to that in the binary material, was observed. The maximum strength was attained at 800 °C for TiAlCr.

Fractographical investigations carried out on the room-temperature fracture specimens of TiAlCr showed a dominant transgranular-cleavage-type fracture (Fig.5a). Lamellar-type fracture regions were also observed in the room-temperature fracture surfaces representing the starting microstructure which contained some regions of lamellar grains (Fig. 5b). Lamellar-type fracture regions were also observed similar to the room temperature fracture surfaces in the specimens fractured at 400 °C. Grain-boundary cracking (Fig. 5c) was predominant at 600 °C and void-nucleation sites were also observed (Fig. 5d). For the TiAlCr also, the specimens tested at 800 and 1000 °C did not fracture. But, fracture surfaces of the specimens bent at these temperatures and subsequently fractured at room temperature were characterized by dominant dimple-fracture regions (Fig. 5e).

3.2. Fracture toughness

3.2.1. *TiAl*

The relationship between fracture toughness, J_{Ic}, and temperature is shown in Fig. 6. The room-temperature toughness was very low and increased with temperature up to 800 °C. Apparent fracture-toughness K_c-values were calculated from the maximum fracture load and net specimen thickness, and they were plotted against the test temperature (Fig. 7). A linear increase in the fracture toughness was observed up to 800 °C and thereafter it decreased. Room-temperature-fracture-toughness K_Q-values were estimated using non-side-grooved specimens. The three specimens tested yielded an average value of 12.7 MPa m$^{1/2}$, which was almost identical to the value obtained using the side-grooved specimen.

Microfractographs of TiAl toughness specimens are shown in Fig. 8. Room-temperature fracture surfaces exhibited an entirely transgranular-cleavage type of fracture with typical "river-patterns" (Fig. 8a). The specimens fractured at 600 °C exhibited a dominant transgranular-cleavage mode of fracture with some

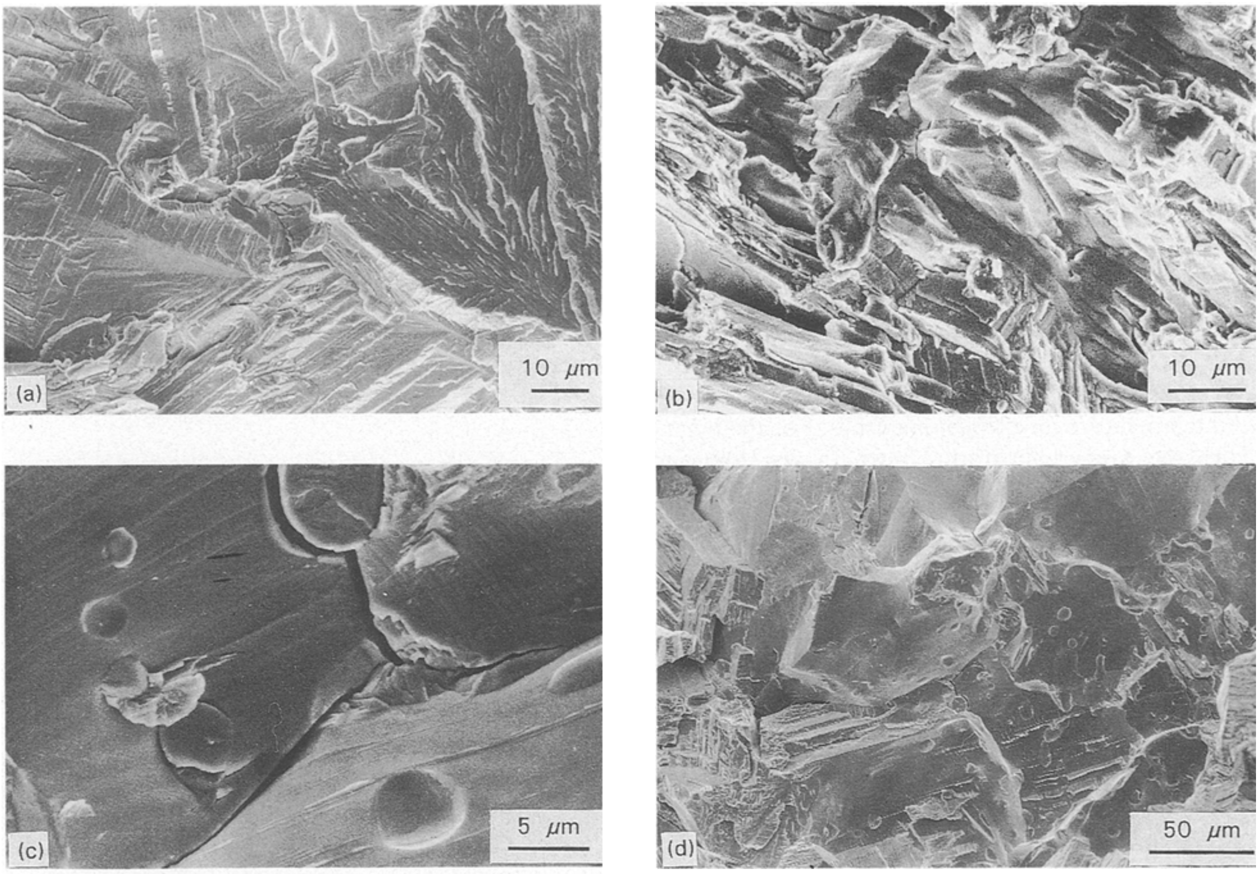

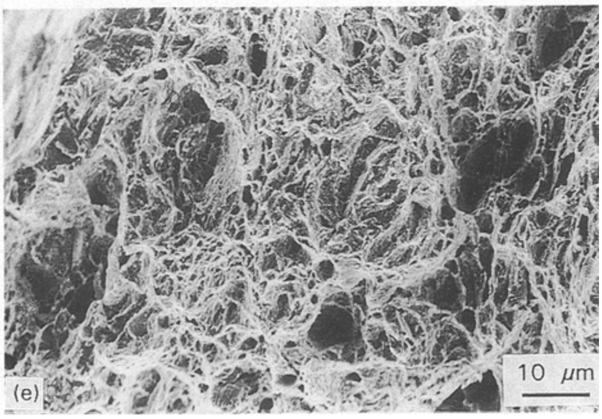

Figure 5 SEM fractographs of TiAlCr bend specimens: (a) 20 °C, (b) 20 °C, (c) 600 °C, (d) 600 °C, and (e) 800 °C.

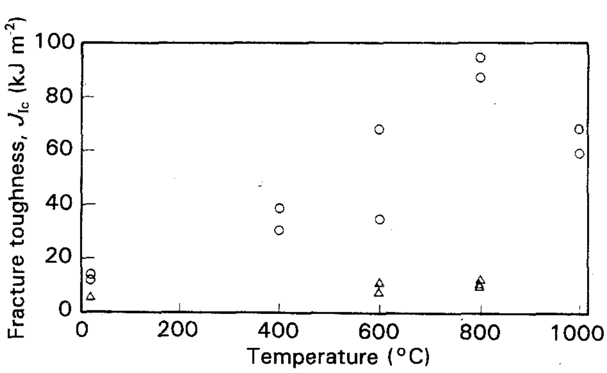

Figure 6 Fracture toughness, J_{Ic} versus temperature for the test materials: (△)TiAl, and (○) TiAlCr.

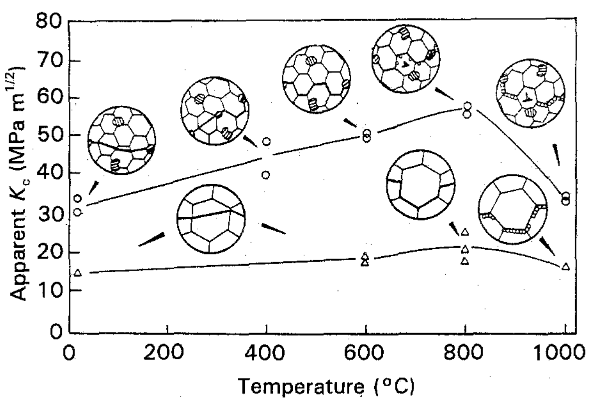

Figure 7 Apparent fracture toughness, K_c versus temperature for test materials with a schematic of the dominant fracture mode: (△) TiAl, and (○) TiAlCr.

intergranular-fracture regions (Fig. 8b). Slip-plane fracture with saw-toothed zigzag planes was also observed (Fig. 8c). With a further increase in the test temperature, the area of the intergranular-fracture region increased. The specimens tested at 1000 °C exhibited an intergranular type of fracture in addition to dimple fracture (Fig. 8d). With increasing temperature, the fracture mode changed from a dominant transgranular cleavage at room temperature to an intergranular mode of fracture at intermediate temperatures. At higher temperatures, dimple fracture was dominant.

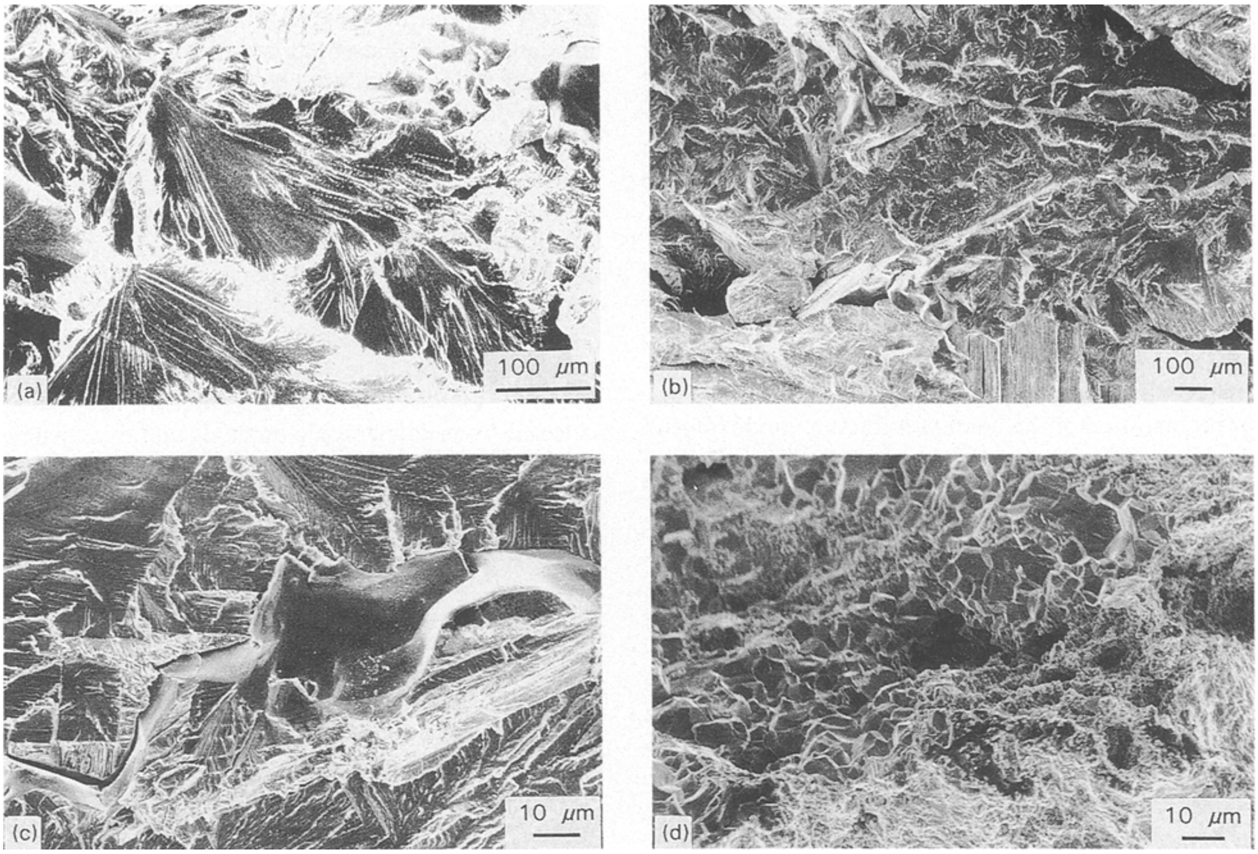

Figure 8 SEM fractographs of TiAl toughness specimens: (a) 20 °C, (b) 600 °C, (c) 600 °C, and (d)1000 °C.

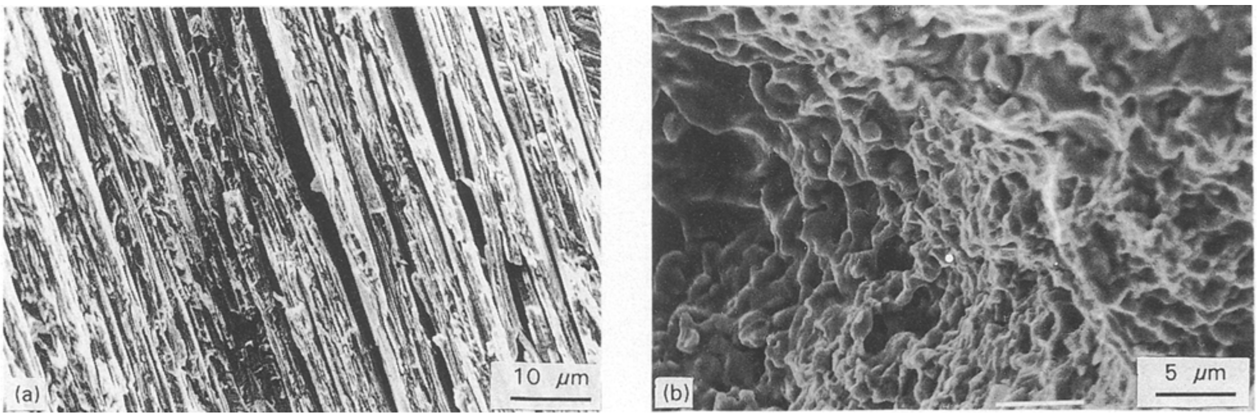

Figure 9 SEM fractographs of TiAlCr toughness specimens: (a) 20 °C and (b) 1000 °C.

3.2.2. TiAlCr

Side-grooved specimens were used to evaluate the fracture-toughness values at room and elevated temperatures and the estimated J_{Ic}-values are shown in Fig. 6. The room temperature toughness of TiAlCr was very high compared to that of binary TiAl. With an increase in temperature, the fracture toughness increased up to a temperature of 800 °C and thereafter it decreased.

Fractographs of the TiAlCr toughness specimens are shown in Fig. 9. Room-temperature fracture was predominantly by transgranular cleavage with typical "river patterns", similar to that shown in Fig. 5a and some lamellar fracture regions were also observed (Fig. 9a). The area of the intergranular-fracture regions increased with increasing temperature. The fracture mode changed to void nucleation, growth and coalescence above 800 °C and the material showed the highest toughness at this temperature (Fig. 9b).

4. Discussion

The mechanical properties measured for TiAl and TiAlCr increased with temperature up to a transition temperature and thereafter they decreased. The detailed fractographical investigations carried out indicate the different fracture modes at different temperatures. The increase in strength and toughness with temperature can be related to the fracture mechanism and is discussed in the following section. Addition of chromium substantially increased the flexural strength and fracture toughness of titanium aluminides. The improvement in the mechanical properties due to addition of chromium can be attributed to various reasons and these are also discussed.

4.1. Fracture mechanisms at elevated temperatures

4.1.1. *TiAl*

Based on fractographical observations, the schematic representation of the dominant fracture mode of bend and toughness specimens are shown in Figs 3 and 7 respectively. For the binary TiAl, room temperature fracture was predominantly by transgranular cleavage with typical "river patterns". It was difficult to differentiate between the fatigue-precrack and the unstable-fracture region because of the brittle nature of failure and the large grain size of the material. Lipsitt and co-workers [10, 11] have investigated the deformation substructure of TiAl up to 900 °C, and they suggested that the mobility of the $a/6[1\,1\,2]$ partial dislocation controls the plasticity of TiAl. This partial dislocation, which is a constituent of the $a\langle 0\,1\,1\rangle$ superdislocation, is immobilized below 700 °C by an unknown obstacle. A large number of microcracks were observed in the unstable-fracture region indicating that the failure mechanism is by microcrack initiation and unstable growth in contrast to the microvoid nucleation, growth and coalescence in the case of conventional titanium alloys [20]. Microcracks might have nucleated in the stress-concentrated-dislocation pile-up sites. The low room-temperature toughness of binary TiAl can be attributed to the poor ductility caused by dislocation interlocking and pile-ups [10, 11].

Above 700 °C the $a/6[1\,1\,2]$ is no longer pinned, and the activity of the $a\langle 0\,1\,1\rangle$ superdislocations increases rapidly with increasing temperature [10, 11]. Twins play an important role in the deformation above 700 °C because the $a/6\langle 1\,1\,2\rangle$ partial dislocation is also the twinning dislocation. During the present investigations, cross-slips or twins were observed in the fracture of bend specimens tested at 600 °C (Fig. 4b). But, no twins were observed in the toughness specimens fractured at same temperature. A sharp fatigue precrack in the toughness specimens increases the crack-tip stresses substantially and promotes cleavage failure. So, the increased brittle nature of failure was observed in the toughness specimens. The fracture surfaces were characterized by transgranular cleavage and slip-plane fracture with saw-toothed zigzag planes (Fig. 8c). Some regions of intergranular fracture were also observed.

Bend specimens tested above 800 and 1000 °C did not fracture. Specimens tested at 800 and 1000 °C, and fractured at room temperature, represented the room-temperature fracture modes. In the toughness TiAl specimens, intergranular-fracture regions were observed at 800 °C in addition to the transgranular-cleavage-fracture regions. The flexural strength was found to decrease at 800 °C compared to the strength at 600 °C. The test material might have possessed maximum flexural strength and fracture toughness in between 600 and 800 °C. The fracture mode changed from a dominant transgranular cleavage to an intergranular mode of fracture at this temperature. The increase in mobility of the dislocations caused an increase in ductility and thus an increase in the toughness of the material.

Though grain-boundary separation was dominant at 1000 °C, dimple-fracture regions were also observed. The increase in the ductility above the brittle–ductile transition temperature is normally attributed to *dynamic recrystallization* [21]. This phenomena is readily detected by metallographic methods and is evidenced by the decrease in hardness [22] and strength and by the increase in ductility. Recrystallization is one reason for the softening of the material at 1000 °C and for the decrease in the toughness, K_c.

4.1.2. *TiAlCr*

In addition to the increase in the measured mechanical properties due to addition of chromium, the temperature at which the maximum strength was obtained was also found to increase. The maximum strength was observed near 600 °C for binary TiAl while it was between 700 and 800 °C for TiAlCr.

The room-temperature fracture surface of the chromium-alloyed material was more or less similar to that of the binary material. But, lamellar-type fracture regions were observed in TiAlCr (Fig. 9a). The increased amount of lamellar grains in TiAlCr might have caused these lamellar fracture regions. The large amounts of energy consumed in tearing hard, lamellar, grains and the relaxation of stresses due to microcracking at lamellar-grain boundaries might have resulted in the improved mechanical properties.

Grain-boundary separation was dominant at 600 °C. Cavities or dimples were also observed on the fracture surfaces (Fig. 5c). Generally, it is considered that cavities are nucleated from the second-phase material or point defects [23]. During the present investigations, cavities were observed in the bend TiAlCr specimens tested at 600 °C (Fig. 5c). From the shape and size of the cavities, it is clear that the cavities might have nucleated from the β-phase [17]. The presence of the β-phase in the ternary material might have accelerated the cavity-nucleation process at lower temperature than for the binary material.

With further increases in temperature, the concentration of cavities considerably increased, and at 1000 °C the specimen exhibited entirely dimple-like fracture. The maximum strength was observed near 700 °C and the maximum toughness at 800 °C. The fracture mode changes from a dominant intergranular fracture to dimple-like fracture near this transition temperature.

4.1.3. *A model for fracture-mode transition*

From the foregoing results and discussion, a model to explain the temperature dependency of the fracture

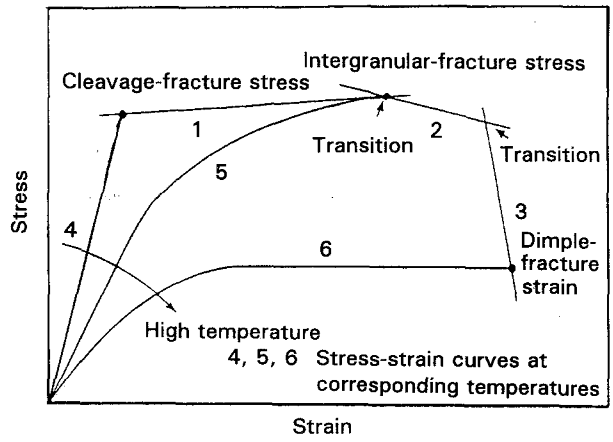

Figure 10 Schematic representation of the dominant fracture mechanism for titanium aluminides.

modes can be proposed as shown in Fig. 10. At lower temperatures, the deformation is interrupted by the occurrence of cleavage fracture. The criterion for cleavage fracture is given by the stress [24], and is indicated by line 1 in Fig. 10. Although the critical cleavage-fracture stress is almost independent of the temperature in steels [24], it depends on the temperature in TiAl-system intermetallic compounds. The critical cleavage-fracture stress increases with increasing temperature due to the increase in the mobility of dislocations, which relax the stress concentration in grains. At higher temperatures, since the grain-boundary cohesive strength decreases with increasing temperature, the critical intergranular-fracture stress (line 2 in Fig. 10) becomes lower than the critical cleavage-fracture stress. There is a rather wide transition region between these two different modes. The maximum value of the strength is observed in the transition region. At even higher temperatures, the deformation is interrupted by the occurrence of dimple fracture. The criterion for ductile dimple fracture is given by the strain [25], and this is shown by line 3 in Fig. 10. Another transition in the fracture mode from intergranular fracture to ductile dimple fracture is observed.

It should be noted from the model proposed here that the different factors corresponding to the fracture modes should be taken into consideration in the improvement of the strength, the fracture toughness and the transition temperature.

4.2. Effects of chromium addition

A substantial improvement in flexural strength and toughness was obtained by the addition of chromium, regardless of the fracture modes and temperatures. The improvement in these properties can be related to the microstructure and crystal structure, which are affected by the addition of chromium, though many other parameters (such as grain size and atomic bonding), may also have some influence.

4.2.1. Microstructure

The room-temperature fracture surfaces were characterized by a lamellar-type fracture in addition to cleavage fracture with "river-patterns" whereas the dominant fracture was of a transgranular-cleavage type in the binary material. The increase in the amount of lamellar grains in TiAlCr results in lamellar fracture regions. Lamellar microstructures increase the crack-growth resistance and thereby increase the toughness of the material [26, 27]. The TiAlCr was also found to have a β-phase in addition to an α_2-phase and a γ-phase [17]. The influence of the β-phase in Ti_3Al–Nb alloys was studied in detail by many investigators; the toughness of the material originated from the ductile β-phase [28]. The high resistance to fracture of the hard α_2-phase and/or the presence of a transformed ductile β-phase [17] contributed to the improved fracture toughness of the TiAlCr alloy investigated.

In addition, many investigators have shown that two-phase materials are more ductile than single-phase titanium aluminides [7, 29, 30]. Huang and Hall [7] and Vasudevan *et al.* [29] have discussed the effect of the α_2-phase on the ductility of TiAl. Since, the α_2-phase dissolves more interstitials (Table I), such as nitrogen and oxygen, than the γ-phase, the increase in the α_2-phase takes more interstitials from the γ-phase and thereby increases dislocation mobility. Addition of chromium strengthens and stabilizes the α_2-phase [30] and permits easy mobility of dislocations. This increase in mobility of dislocations also contributes to the improvement in toughness.

4.2.2. Crystal structure

The increase in the mechanical properties measured can be related to the crystal structure of the material [31, 32]. The unit cell of TiAl has a face-centred tetragonal (f.c.t.) structure with a c/a ratio greater than unity [33]. Sastry and Lipsitt [34] have studied the deformation behavior of TiAl and they attributed the poor ductility to the inactive slip system. But, addition of ternary elements reduced the unit-cell volume and the c/a ratio considerably [35, 36]. Plastic deformation becomes easier, and it might have resulted in the increased toughness of the chromium-alloyed material.

The above discussion is related mainly to the cleavage fracture. There is little information available about intergranular fracture and ductile dimple fracture of TiAl alloys at elevated temperatures. Further detailed investigation is needed to comprehend the dominant factor in the improvement of the strength and fracture toughness of chromium-alloyed TiAl at elevated temperatures.

5. Conclusions

Flexural-strength and fracture-toughness experiments were carried out at different temperatures on TiAl and TiAlCr, and the fracture mechanisms were investigated. The results can be summarized as follows.

1. The flexural strength and fracture toughness of the binary and ternary materials increased up to a transition temperature and thereafter they decreased.

There was an increase in the transition temperature at which the strength and fracture toughness decrease; this was due to the addition of chromium.

2. Addition of chromium improved the flexural strength and fracture toughness of γ-phase titanium aluminides. The α_2-phase and β-phase present in chromium-alloyed titanium aluminide contribute positively to the flexural strength and fracture toughness.

3. The fracture mechanism at elevated temperatures is affected by the addition of chromium. Dimple fracture was observed in the ternary material at a lower temperature than in the binary material.

4. The fracture mode and fracture mechanism changed with temperature. The various factors corresponding to the fracture modes should be taken into consideration of improvements in the strength and toughness.

Acknowledgements
The authors acknowledge the technical comments provided by Dr T. Hanamura and Mr Y. Mizuhara of the Nippon Steel Corporation and also acknowledge the experimental assistance of Mr N. Miyahara of Nagaoka University of Technology. The support for one of the authors (RG) from the Japanese Ministry of Education, Science and Culture is gratefully acknowledged.

References

1. H. A. LIPSITT, *Mater. Res. Soc. Symp. Proc.* **39** (1985) 351.
2. G. SAUTHOFF, *Z. Metallkde* **80** (1989) 337.
3. Y. M. KIM, *J. Metals* **41** (1989) 24.
4. S. C. HUANG and E. L. HALL, *Met. Trans. A* **22** (1991) 2619.
5. T. HANAMURA, R. UEMORI and M. TANINO, *J. Mater. Res.* **3** (1988) 656.
6. S. C. HUANG and E. L. HALL, *Acta Metall.* **39** (1991) 1053.
7. *Idem., Met. Trans. A* **22** (1991) 427.
8. T. TSUJIMOTO and K. HASHIMOTO, in "High temperature ordered intermetallic alloys III", Material Res. Soc. Symp. Proc., edited by C. C. Koch, N. S. Stoloff, C. T. Liu and A. I. Taub, (Mater. Res. Soc., Pittsburg, PA, 1989) **133** p. 391.
9. S. A. COURT, V. K. VASUDEVAN and H. L. FRASER, *Phil. Mag. A.* **61** (1990) 141
10. H. A. LIPSITT, D. SCHECHTMAN and R. E. SCHAFRIK, *Met. Trans. A* **6** (1975) 1991.
11. D. SCHECHTMAN, M. J. BLACKBURN and H. A. LIPSITT, *ibid. A* **5** (1974) 1373.
12. G. HUG, A. LOISEAU and A. LASALMONIE, *Phil. Mag. A.* **54** (1986) 47.
13. ASTM E399-81, in "1981 Annual Book of ASTM Standards", Part 10, (American Society of Testing Materials, Philadelphia, 1981) p. 592.
14. T. KAWABATA, T. TAMURA and O. IZUMI, *Mater. Res. Soc. Symp. Proc.* **133** (1989) 324.
15. M. NOBUKI, K. HASHIMOTO, J. TAKAHASHI and T. TSUJIMOTO, *Mater. Trans., JIM* **31** (1990) 814.
16. ASTM E813-81, in "1981 Annual Book of ASTM Standards", Part 10 (American Society of Testing Materials, Philadelphia, 1982). p. 822.
17. T. HANAMURA, N. MASAHASHI, Y. MIZUHARA, M. MATSUO and K. MIYASAWA, in Proceedings of the Spring Meeting of Japan Institute of Metals, March 31–April 12, 1992, Cheba, Japan (1992) p. 320.
18. Y. MUTOH, in "Role of fracture mechanics in modern technology" (Elsevier Science, 1987) p. 503.
19. Y. MUTOH, I. SAKAMOTO and S. TAKEDA, *Trans. Jpn Soc. Mech. Eng., Ser. A.* **55** (1989) 1613.
20. D. A. LUKASAK and D. A. KOSS, *Met. Trans. A* **21** (1990) 135.
21. P. G. SHEWMON, in "Transformations in metals" (McGraw-Hill, New York, 1969).
22. R. GNANAMOORTHY and Y. MUTOH, unpublished results.
23. G. E. DIETER, "Mechanical metallurgy" (McGraw-Hill, Tokyo, 1984) p. 232.
24. J. F. KNOTT, "Fundamentals of fracture mechanics" (Butterworths London, 1974) p. 188.
25. *Idem., ibid.* (Butterworths, London, 1974) p. 204.
26. S. L. KAMPE, P. SADLER, D. E. LARSEN and L. CHRISTODOULOU, in "Microstructure/property relationships in titanium aluminides and alloys" (The Minerals, Metals and Materials Society, Warrendale, PA, 1991) p. 313.
27. S. TSUYAMA, S. MITAO and K. MINAKAWA, *ibid.* (The Minerals, Metals and Materials Society, Warrendale, PA, p. 213.
28. R. STRYCHOR, J. C. WILLIAMS and W. A. SOFFA, *Met. Trans. A* **19** (1988) 225.
29. V. K. VASUDEVAN, M. A. STUCKE, S. A. COURT and H. L. FRASER, *Phil. Mag. Lett* **59** (1989) 299.
30. W. WUNDERLICH, T. KREMSER and G. FROMMEYER, *Z. Metallkde* **81** (1990) 802.
31. M. J. MARCINKOWSKLI, N. BROWN and R. M. FISCHER, *Acta Metall.* **9** (1961) 129.
32. B. A. GREENBERG, *Phys. Status Solidi* **42** (1970) 459.
33. P. DUWEZ, and J. L. TAYLOR, *Trans. AIME* **194** (1952) 70.
34. S. M. L. SASTRY and H. A. LIPSITT, *Acta Metall.* **25** (1977) 1279.
35. S. C. HUANG and E. L. HALL, *Mater. Res. Soc. Symp. Proc.* **133** (1989) 373.
36. D. VUJIC, Z. LI and S. H. WHANG, *Met. Trans. A* **19** (1988) 2445.

Received 30 July 1992
and accepted 3 June 1993